Figures and figure supplements

Caenorhabditis elegans PIEZO channel coordinates multiple reproductive tissues to govern ovulation

Xiaofei Bai *et al*

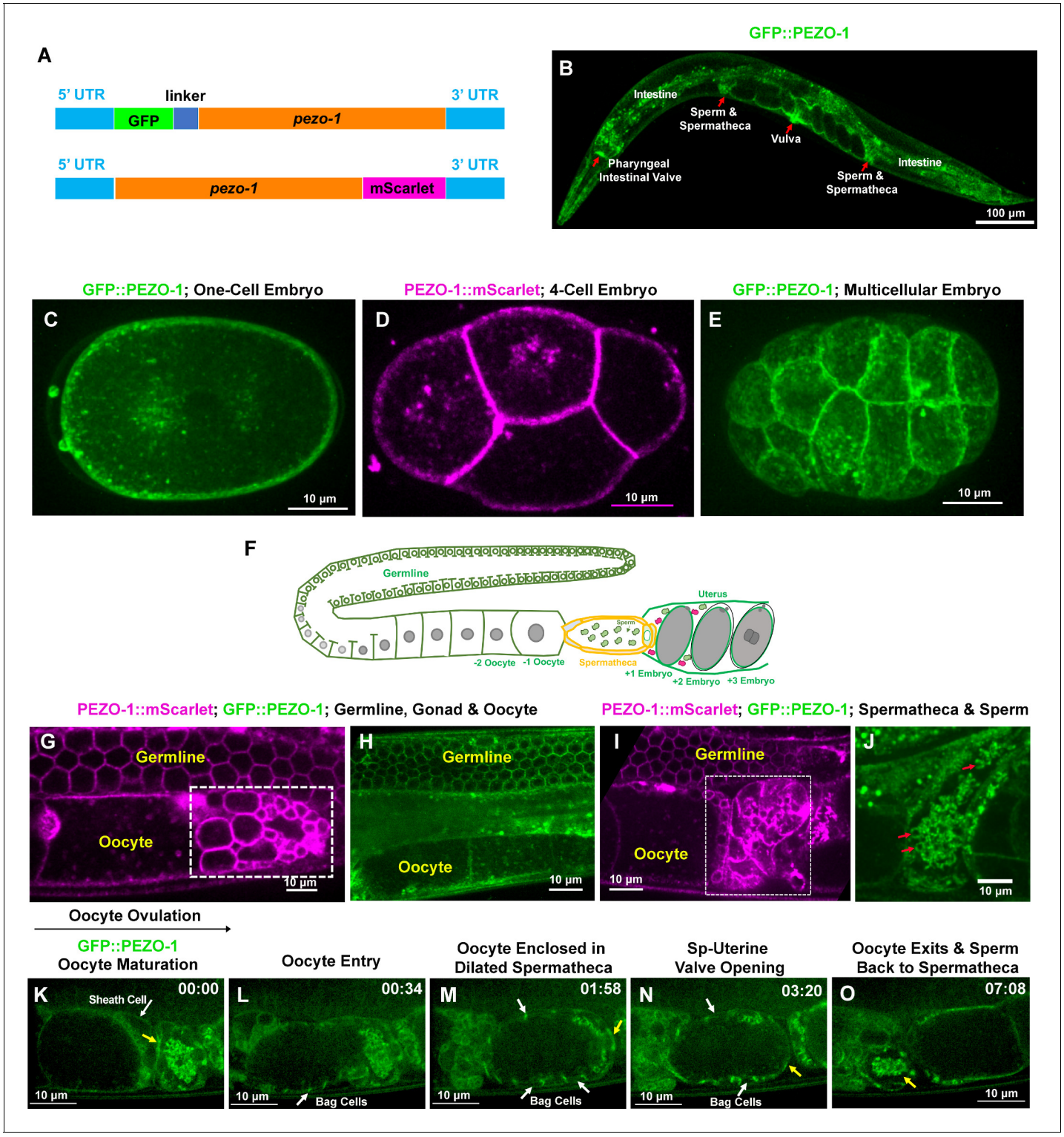

Figure 1. *pezo*-1 is widely expressed in *C. elegans*. (**A**) Two fluorescent reporter genes were knocked-in to both N-terminus and C-terminus of *pezo-1*. (**B**) GFP::PEZO-1 is strongly expressed in multiple mechanosensitive tissues, such as the pharyngeal-intestinal valve, spermatheca, and vulva (red arrows). (**C, E**) GFP::PEZO-1 (green) is expressed in the plasma membrane of different-staged embryos. (**D**) PEZO-1::mScarlet (magenta) also localizes to the plasma membranes of embryos. (**F**) A schematic of the *C. elegans* gonad. (**G–J**) Both PEZO-1::mScarlet (magenta) and GFP::PEZO-1 (green) localize to reproductive tissues, such as the plasma membranes of the germline cells (**G–I**), somatic gonad (**G–J**), spermatheca (I; in white box), and sperm (J; red arrows). PEZO-1::mScarlet (magenta) also labels the spermatids that have not yet migrated into the spermatheca (small circles, white box in

Figure 1 continued on next page

Figure 1 continued

panel [G]) and the residual bodies not yet engulfed by the sheath cells (bigger circles, white box in panel [G]) (***Huang et al., 2012***). (**K–O**) Representative images of PEZO-1 localization during ovulation and fertilization. GFP::PEZO-1 (green) localizes to the sheath cell (white arrow) and the spermathecal distal valve (yellow arrow (**K**), which remains closed before ovulation. The oocyte is ovulated, enters into the spermatheca (**L**) and remains enclosed in the spermatheca until fertilization is completed (**M**). During fertilization, GFP::PEZO-1 remained on the spermathecal-uterine (sp-ut) valve as indicated by a yellow arrow (**M, N**). The bag cells of the spermatheca also express GFP::PEZO-1 at this time (representative bag cells are marked by white arrows in panels (**L–N**). After fertilization, the sp-ut valve opened (N, yellow arrow) and allowed the newly fertilized zygote to exit the constricting spermatheca (**N, O**). Constriction of the spermatheca pushes the fertilized zygote into the uterus; sperm can be seen in the constricted spermatheca (O, yellow arrow). The black arrow above panel (K) shows the direction of embryo travelthrough the spermatheca from left to right. The timing of each step is labeled on the top right in minutes and seconds. Scale bars are indicated in each panel.

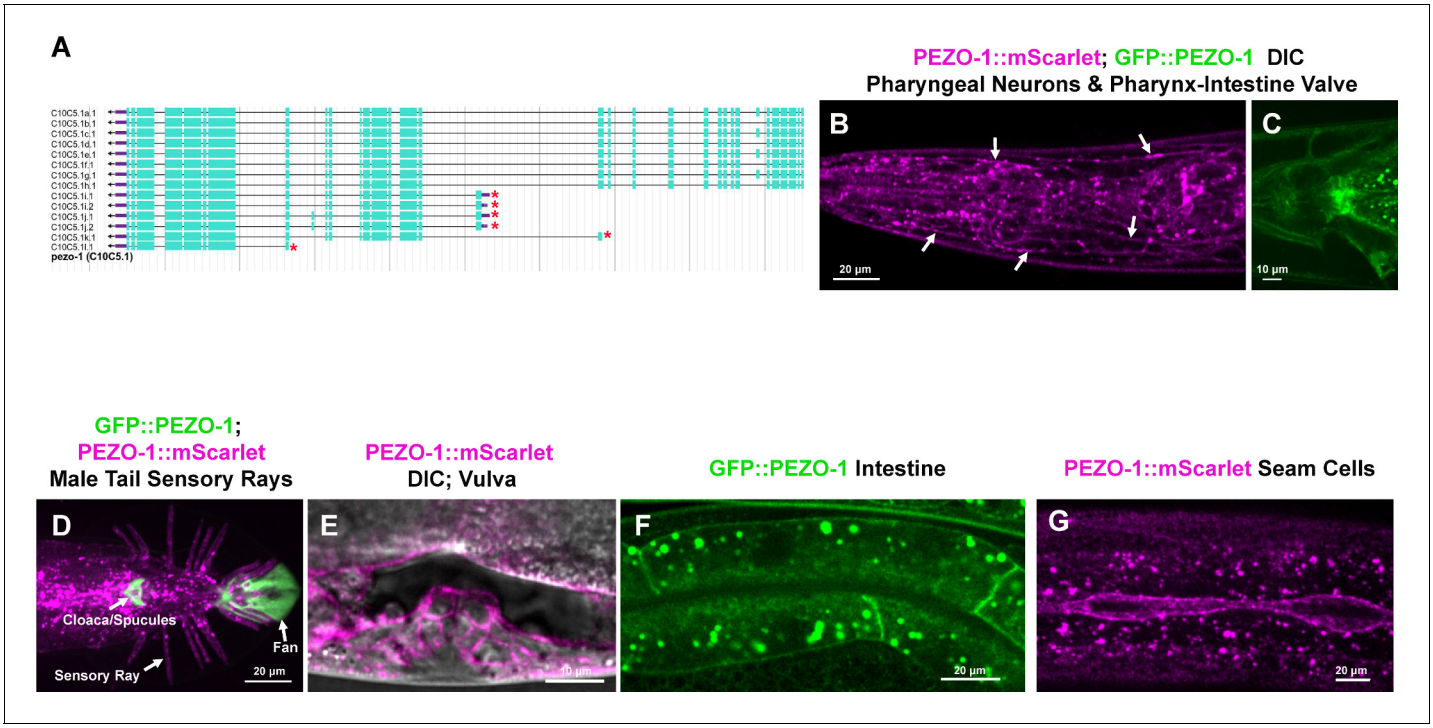

Figure 1—figure supplement 1. PEZO-1 is expressed in multiple tissues throughout development. (**A**) There are 14 mRNA isoforms encoded by *pezo-1*. Isoforms i-l encode the six short forms of *pezo-1* (red asterisks). The 5′−3′ orientation is right to left. (**B–G**) Both PEZO-1::mScarlet (magenta) and GFP::PEZO-1 (green) express in a variety of cell types, including pharyngeal neurons (panel [B], white arrows), pharyngeal-intestinal valve (**C**), male tail, including sensory rays (magenta), fan (green), cloaca/spicules (green) (**D**), vulva (**E**), intestinal cells (**F**) and seam cells (**G**). Scale bars are shown in each panel. The illustration in panel (A)was taken from WormBase (https://wormbase.org).

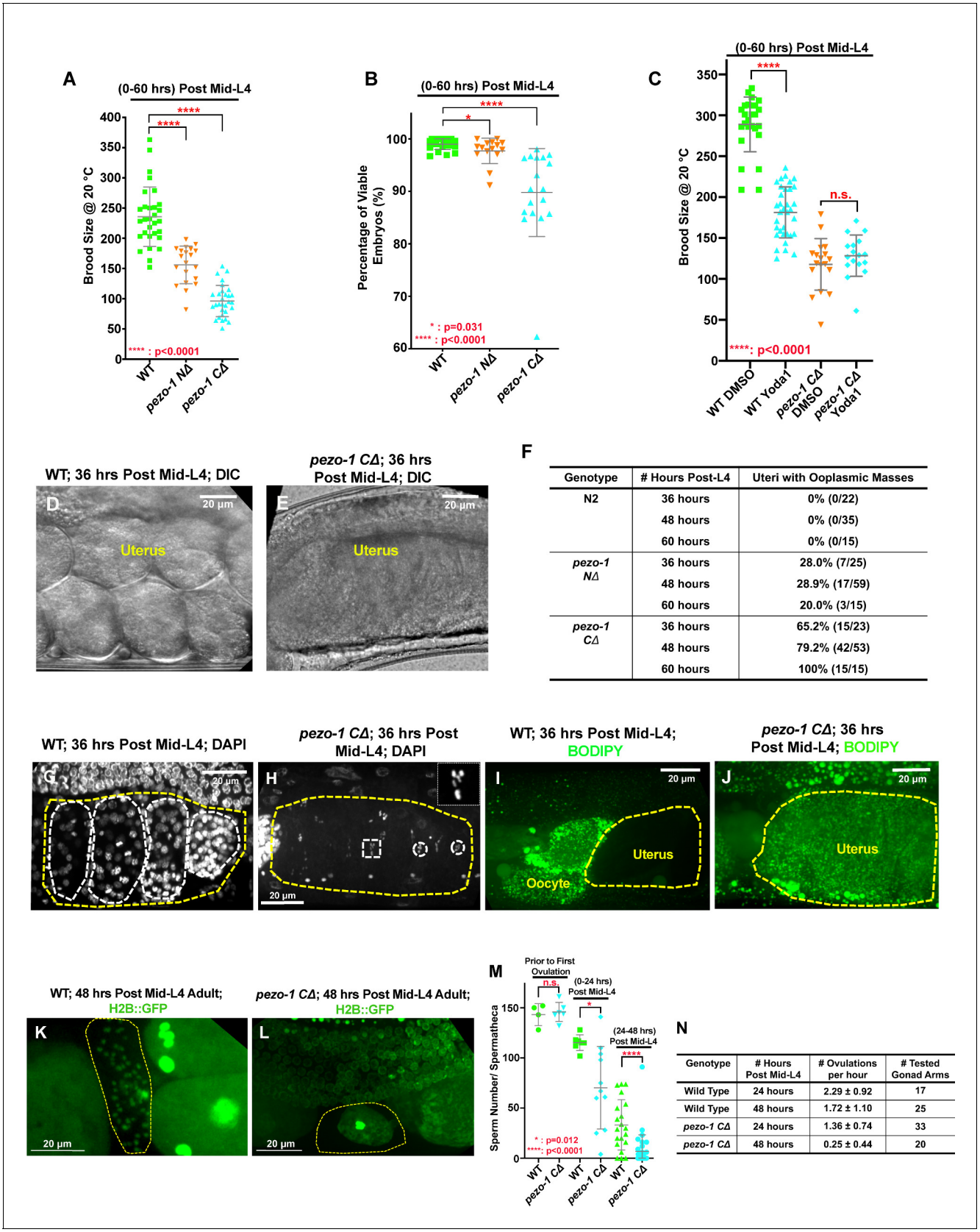

Genotype	# Hours Post-L4	Uteri with Ooplasmic Masses
N2	36 hours	0% (0/22)
	48 hours	0% (0/35)
	60 hours	0% (0/15)
pezo-1 NΔ	36 hours	28.0% (7/25)
	48 hours	28.9% (17/59)
	60 hours	20.0% (3/15)
pezo-1 CΔ	36 hours	65.2% (15/23)
	48 hours	79.2% (42/53)
	60 hours	100% (15/15)

Genotype	# Hours Post Mid-L4	# Ovulations per hour	# Tested Gonad Arms
Wild Type	24 hours	2.29 ± 0.92	17
Wild Type	48 hours	1.72 ± 1.10	25
pezo-1 CΔ	24 hours	1.36 ± 0.74	33
pezo-1 CΔ	48 hours	0.25 ± 0.44	20

Figure 2. Deletions of the *pezo-1* gene cause a reduction in brood size. (**A**) Brood size was significantly reduced in both *pezo-1 NΔ* and *pezo-1 CΔ* animals when compared with wildtype, and this reduction was most evident in older adult animals. (**B**) The percentage of viable embryos was reduced

Figure 2 continued on next page

Figure 2 continued

in the *pezo-1 C*Δ animals. (**C**) Dietary supplementation of a PIEZO1-channel-specific activator Yoda1 in wildtype animals significantly reduced the brood size compared with control treatment, but brood size was not further reduced in *pezo-1 C*Δ when treated with Yoda1. (**D, E**) DIC images of the uteri of gravid adult animals. Wildtype animals had young embryos in their uteri (**D**), whereas only a large ooplasmic mass was observed in *pezo-1 C*Δ mutant uteri (**E**). (**F**) Quantification of the percentage of uteri with ooplasmic masses in wildtype and *pezo-1* deletion mutants. N2 is the wildtype strain. (**G, H**) DAPI staining demonstrated that multicellular embryos (white circles in panel [**G**]) were present in the uteri of wildtype animals, whereas only oocyte meiotic chromosomes (white circles and rectangle) were observed in the uteri of *pezo-1 C*Δ mutants (panel [H]; inset in the top right white box shows an amplified image of the meiotic chromatin marked with a white rectangle). The yellow dotted lines indicate the boundaries of the uteri in panels (G) and (H). (**I, J**) Only unfertilized oocytes and newly fertilized zygotes are permeable to BODIPY (green) in wildtype (WT) animals (**I**), whereas staining was observed throughout the entire uterine mass (yellow circle in panel [**J**]) of *pezo-1 C*Δ animals. (**K, L**) An H2B::GFP transgene was crossed into our strains to visualize oocyte and sperm chromatin. (**K**) Sperm labeled by H2B::GFP (green cells in yellow circle) reside in the spermatheca (yellow circle) of Day 2 adults (48 hr post mid-L4). (**L**) Only oocyte debris (yellow circle) is left in the spermatheca of an age-matched *pezo-1 C*Δ mutant. (**M**) Quantification of sperm counts in both wildtype and *pezo-1 C*Δ hermaphrodites at different time windows. (**N**) Quantification of the oocyte ovulation rate of wildtype and *pezo-1 C*Δ adults at different ages. The oocyte ovulation rate was significantly reduced in the older *pezo-1 C*Δ mutant adults. P-values: *, p=0.031 (**B**); *, p=0.012(**M**); ****, p<0.0001 (*t*-test).

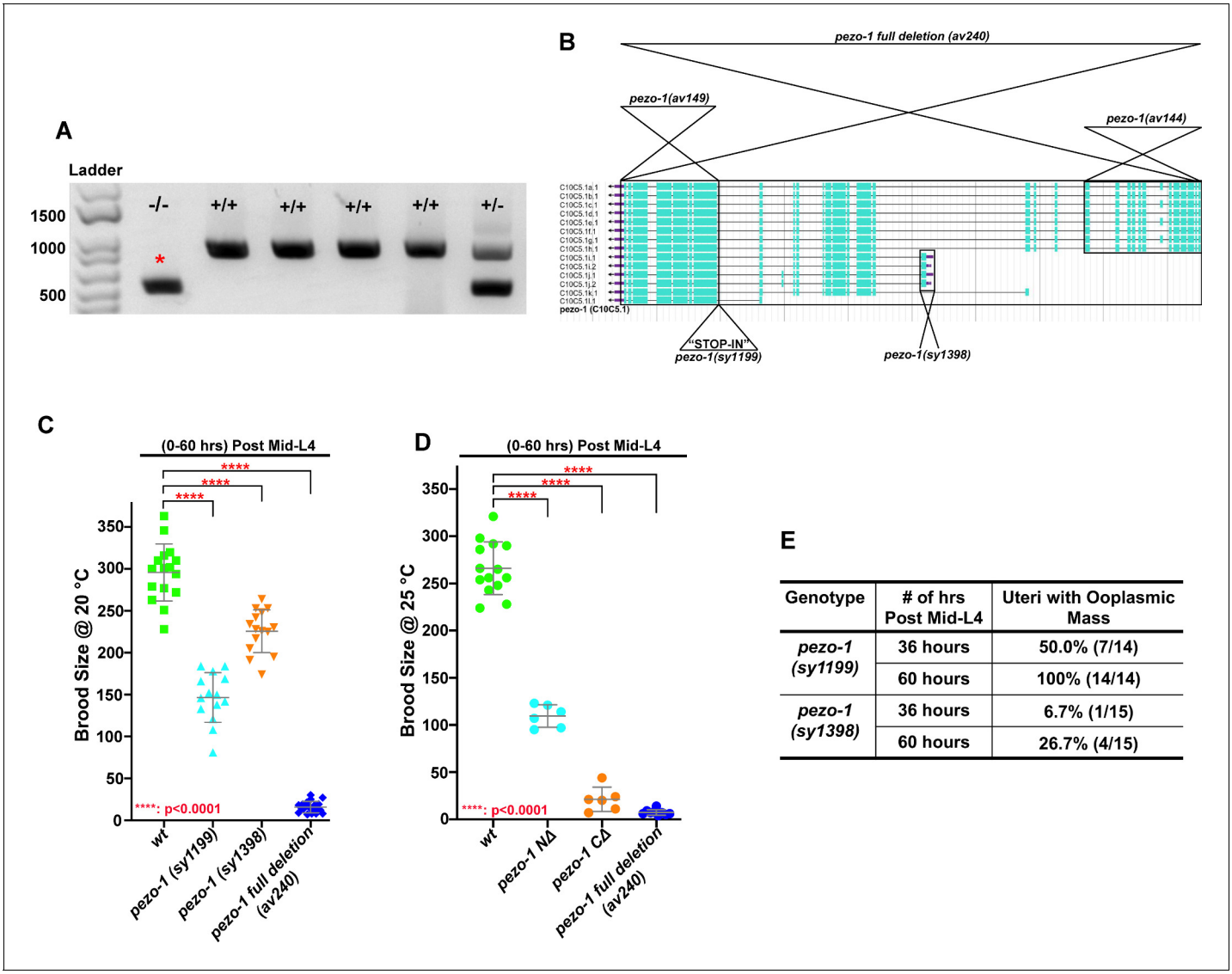

E

Genotype	# of hrs Post Mid-L4	Uteri with Ooplasmic Mass
pezo-1 (sy1199)	36 hours	50.0% (7/14)
	60 hours	100% (14/14)
pezo-1 (sy1398)	36 hours	6.7% (1/15)
	60 hours	26.7% (4/15)

Figure 2—figure supplement 1. Verification of CRISPR/Cas9-generated deletions in *pezo-1* knockout animals. (**A**) Representative PCR gel from genotyping single animals for *pezo-1 CΔ* knockout candidates. A positive homozygous knockout line is labeled with a red asterisk. Three primers (two that flank the deletion and one internal) were used to test the homozygosity of candidate *pezo-1* deletion animals. The amplicon size of a homozygous deletion with both flanking primers is 450-bp (labeled –/–). In the wild type, an 879-bp PCR product was able to be amplified by one flanking primer and the internal primer (labelled +/+). Heterozygous animals contain both of the PCR products (labeled +/–). (**B**) Schematic of the 14 mRNA isoforms and the position of the three deletion alleles used in this study and the isoforms that they should affect. The STOP-IN line is also shown as an insertion in the beginning of exon 27. The 5′−3′ orientation is right to left. (**C**) The full deletion allele and four other alleles generated for this study also had reduced brood sizes: the full deletion mutant *pezo-1(av240)*, a N-terminal mutant *pezo-1(av144)*, a C-terminal mutant *pezo-1(av149)*, a stop-in mutant *pezo-1(sy1199)* and a small deletion allele *pezo-1(sy1398)* in isoforms I and J. (**D**) The reduction in brood size of *pezo-1* deletion animals was enhanced when the animals were grown at 25˚C. (**E**) Quantification of the percentage of uteri with ooplasmic masses in *pezo-1(sy1199)* and *pezo-1(sy1398)* mutants. P-values: ***, p=0.0003 (**C**); **, p=0.0021 (**D**); ***, p=0.0002 (**D**); ****, p<0.0001 (*t*-test). The illustration in panel (B) was taken from WormBase (https://wormbase.org).

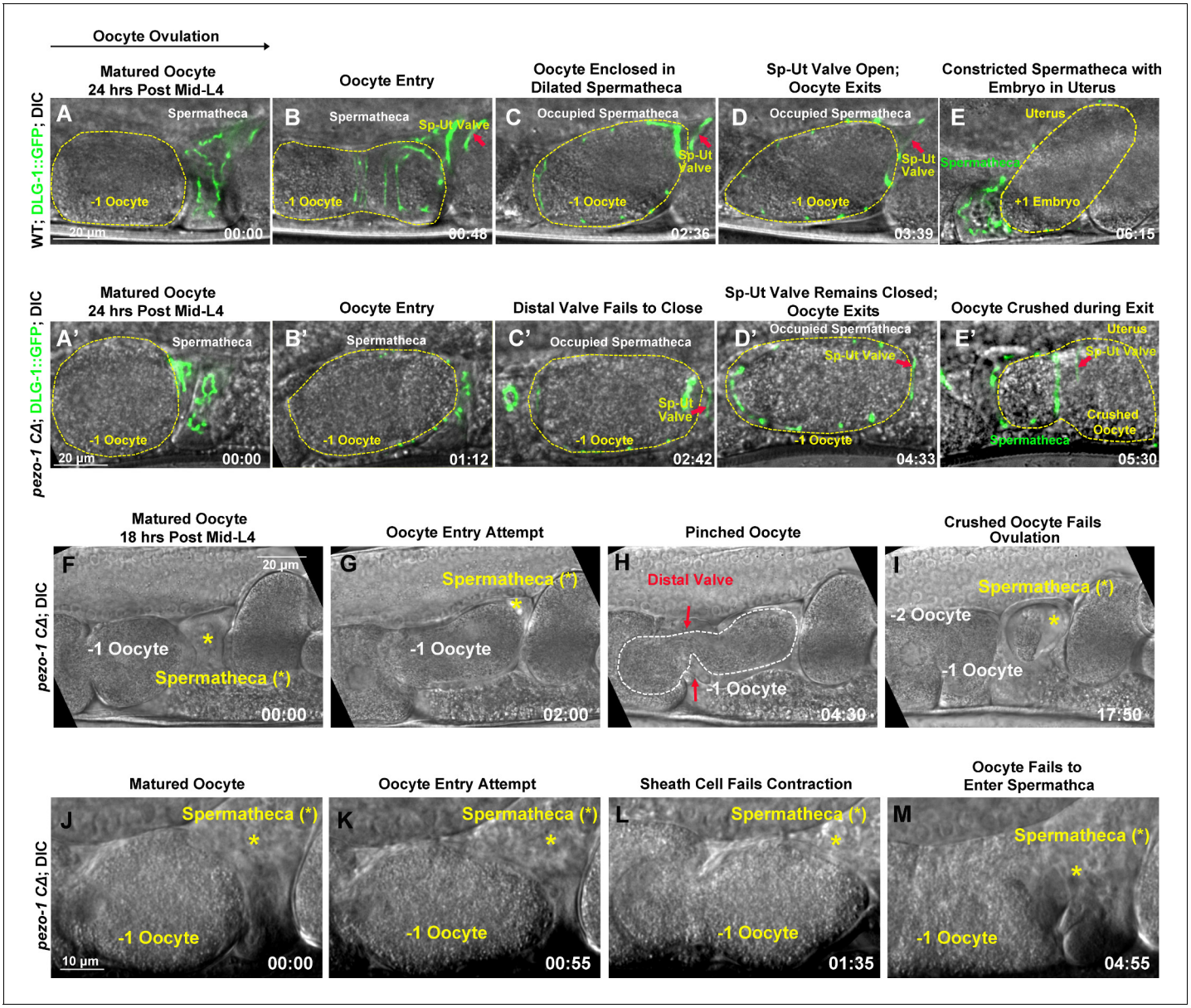

Figure 3. PEZO-1 mutants exhibit severe ovulation defects. (**A–E**) Ovulation in wildtype animals. (**A, B**) Ovulation is initiated by oocyte (yellow dotted circle) entry into the spermatheca, which was labelled by the apical junctional marker DLG-1::GFP (green). (**C**) Fertilization occurs in the occupied spermatheca (yellow dotted circle). (**D, E**) After fertilization, the sp-ut valve (red arrows) opened immediately to allow the newly fertilized zygote (yellow dotted circle) to exit the spermatheca and enter the uterus. (**A′–E′**) Abnormal ovulation was observed in *pezo-1 CΔ* animals. Control of the spermathecal valves was aberrant (**C′–E′**) during ovulation and the DLG-1::GFP labelled sp-ut valve (red arrow) never fully opened; the oocyte was crushed as it was expelled (**E′**). (**F–M**) Two examples of ovulation defects observed in the *pezo-1 CΔ* mutants. (**F–I**) The ovulating oocyte (white dotted circle) was pinched off by the spermathecal distal valve (red arrows in panel [**H**]). This oocyte never exited into the uterus. (**J–M**) *pezo-1 CΔ* oocytes frequently failed to enter the spermatheca and were retained in the oviduct (**M**). The black arrow above panel (A) shows the direction of embryo travel through the spermatheca from left to right. All four image time series follow this same left to right orientation. The timing of each step is labeled on the bottom right in minutes and seconds. Scale bars are shown in each panel.

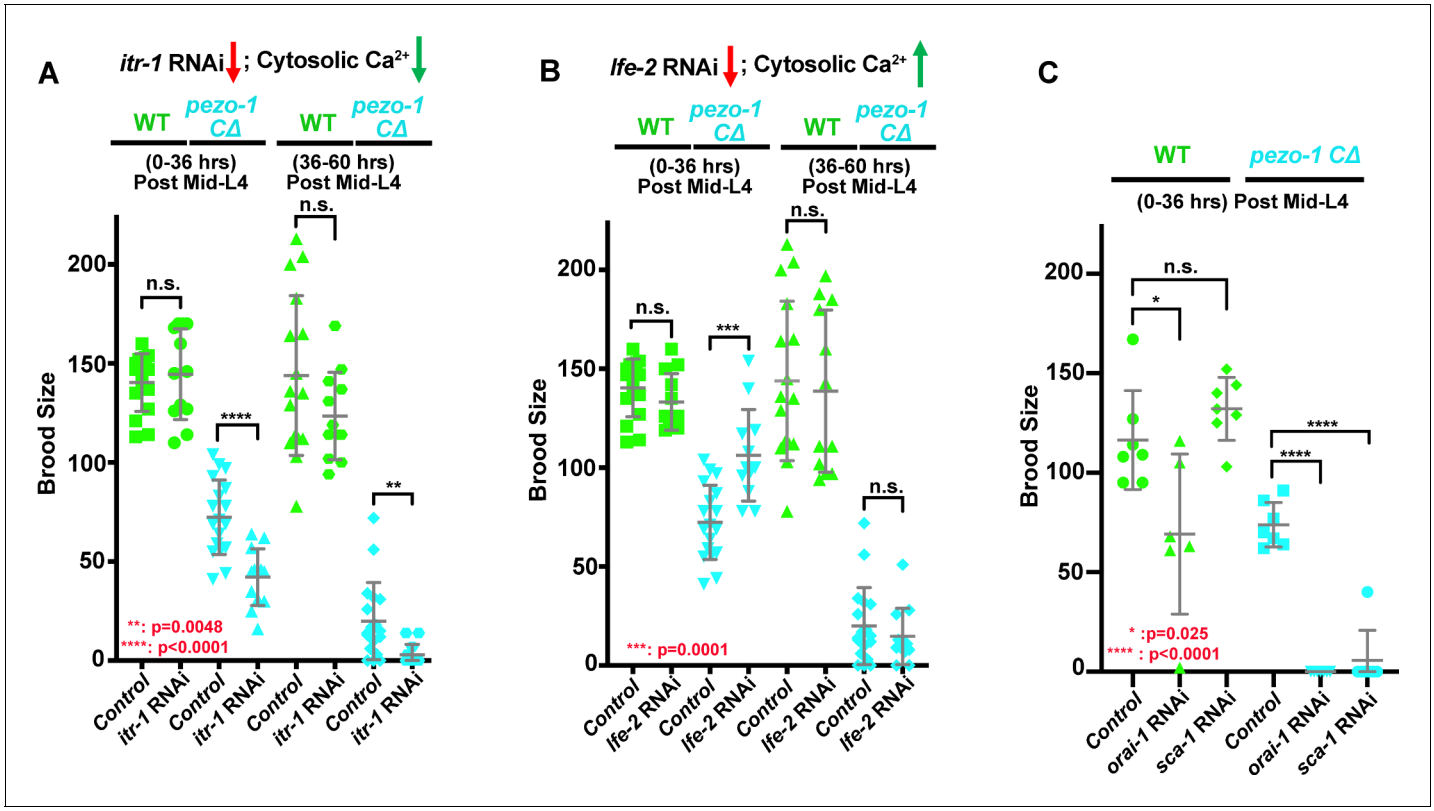

Figure 4. *pezo-1* mutants show genetic interactions with cytosolic Ca^{2+} regulators. (**A**) *itr-1* (RNAi) reduced the brood size in *pezo-1 CΔ* animals. (**B**) By contrast, *lfe-2* (RNAi) slightly rescued the smaller brood size in *pezo-1 CΔ* animals. (**C**) Depletion of both *orai-1* and *sca-1* by RNAi also enhanced the brood size reduction of *pezo-1 CΔ* mutants. P-values: *, p=0.025 (**C**); **, p=0.0048 (**A**); ***, p=0.0001 (**B**); ****, p<0.0001 (*t*-test).

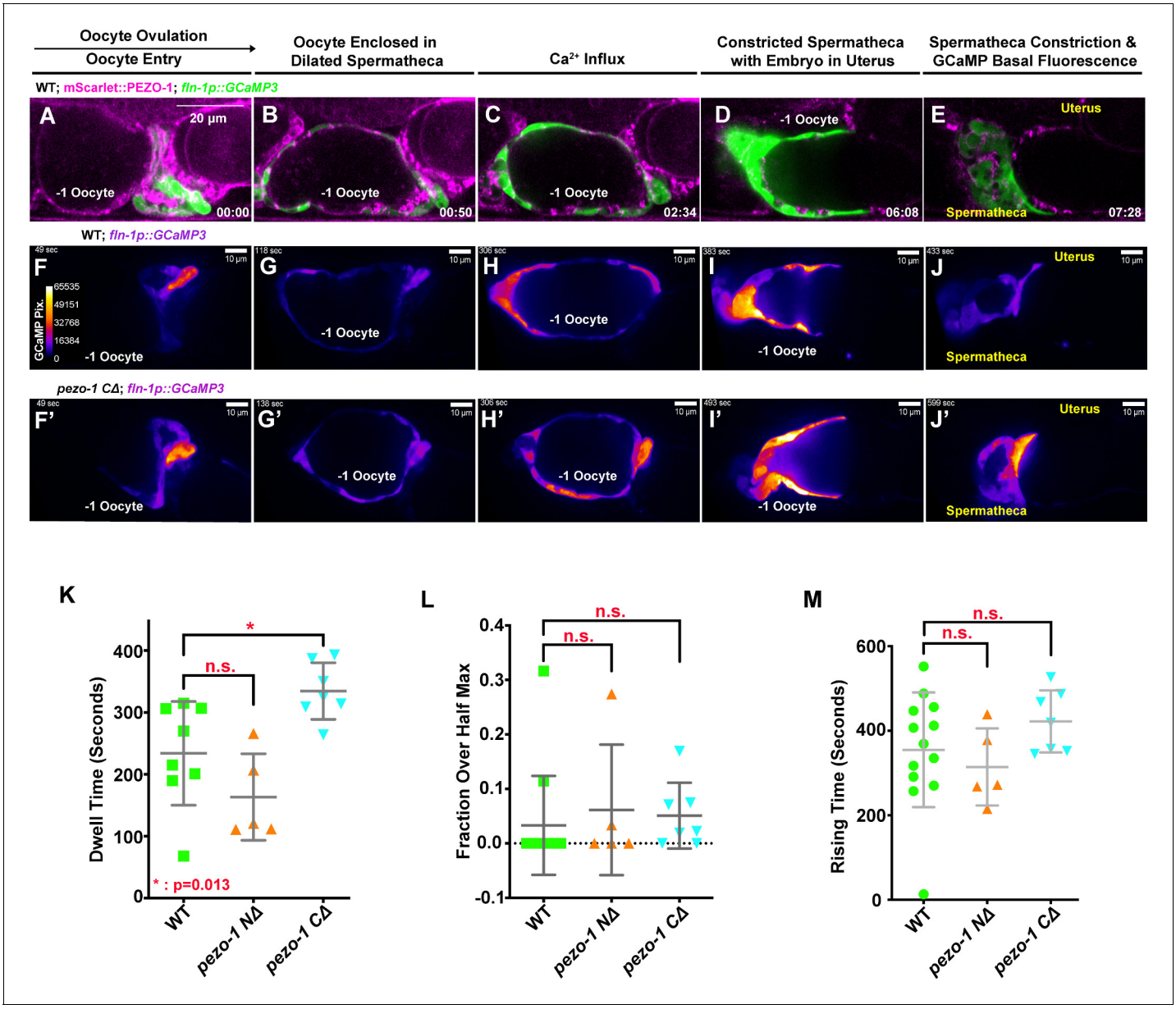

Figure 5. PEZO-1 mutants show normal GCaMP3 fluorescence during ovulation. (**A–E**) mScarlet::PEZO-1 colocalizes with GCaMP3, which is driven by a spermatheca-specific promoter. These images represent the third ovulation for this spermatheca. (**F–J'**) Time series frames from GCaMP3 recordings in the third ovulation of both wildtype animals (**F–J**) and *pezo-1 CΔ* animals (**F'–J'**). Ca^{2+} influx was quantified during ovulation and fertilization, as indicated by the intensity of GCaMP3 pixels (colored bar in panel [F]). (**F, F'**) Oocyte entry into the spermatheca in wildtype and *pezo-1 CΔ*. (**G, G'**) Oocytes in the spermatheca, (**H, H'**) Ca^{2+} influx during fertilization, (**I, I'**) intense Ca^{2+} influx as the sp-ut valve closes to push newly fertilized zygote into the uterus, and (**J, J'**) the return to basal levels as the spermatheca prepares for the next ovulation. (**K**) Dwell time is a tissue function metric calculated as the time the oocyte resides in the spermatheca from the closing of the distal valve to the opening of the sp-ut valve. (**L, M**) Calcium signaling metrics: fraction over half max (**L**) and rising time (**M**) in *pezo-1* mutants showed normal calcium levels during ovulation compared with wild type (***Bouffard et al., 2019***). The black arrow above panel (A) shows the direction of embryo travel through the spermatheca from left to right. All three image time series follow this same left to right orientation. The timing of each step is labeled in the bottom right in minutes and seconds (**A–E**), or on the top left in seconds (**F–J'**). Scale bars are shown in each panel.

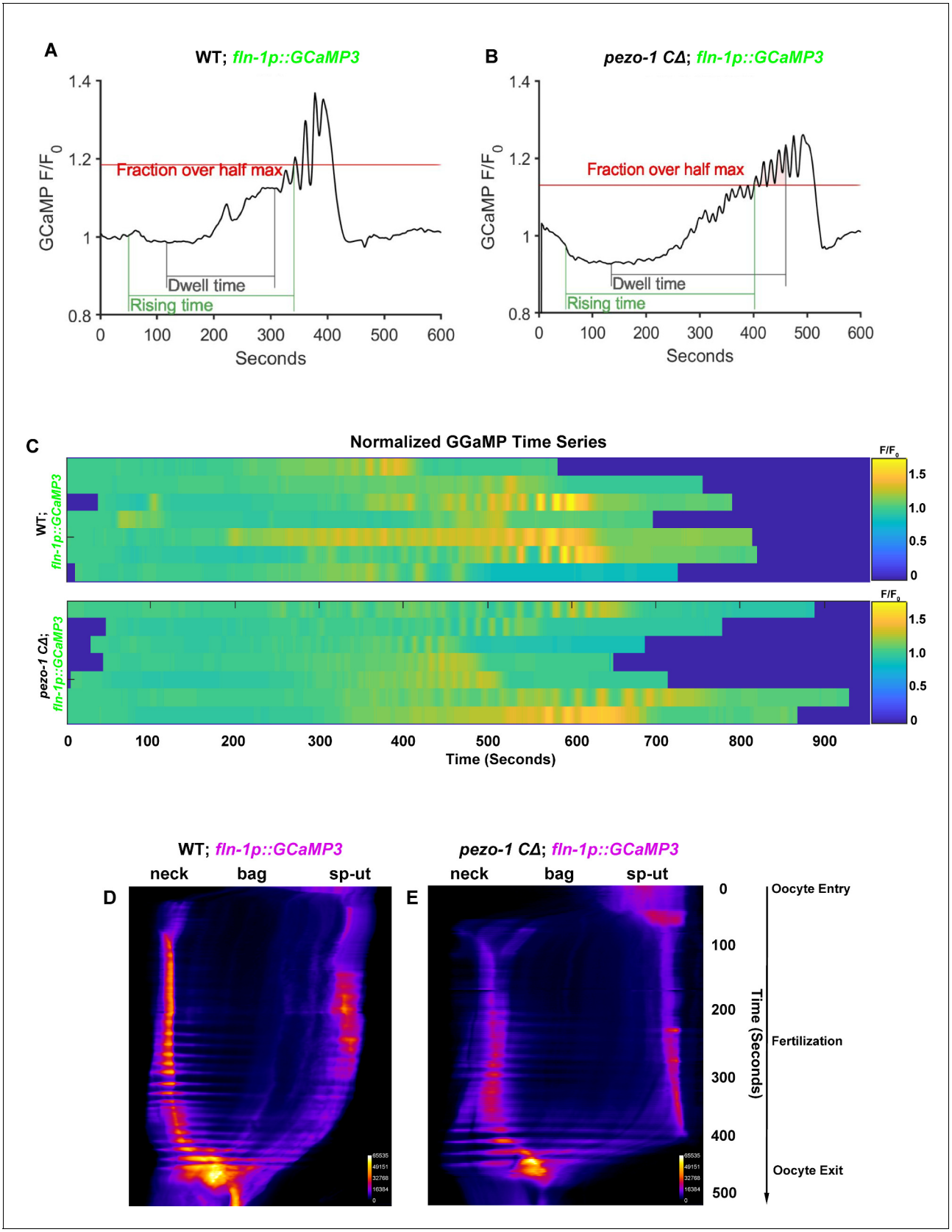

Figure 5—figure supplement 1. Normal calcium signaling was observed in the spermathecal cells in *pezo-1* mutants. (**A, B**) GCaMP3 time series of normalized average pixel intensity from a single oocyte transit recording over the same spatial frame and time. (**C**) Heat map of GCaMP3 normalized

Figure 5—figure supplement 1 continued on next page

Figure 5—figure supplement 1 continued

average pixel intensity (F/F_0) versus time series during ovulation from seven oocyte transit recordings in both wildtype and *pezo-1 CΔ* mutants. Color bar represents the gradient of the normalized average pixel intensity (F/F_0). (**D, E**) Representative kymograms of GCaMP3 in both wildtype and *pezo-1 CΔ* mutants. Color bar represents the gradient of the fluorescence intensity.

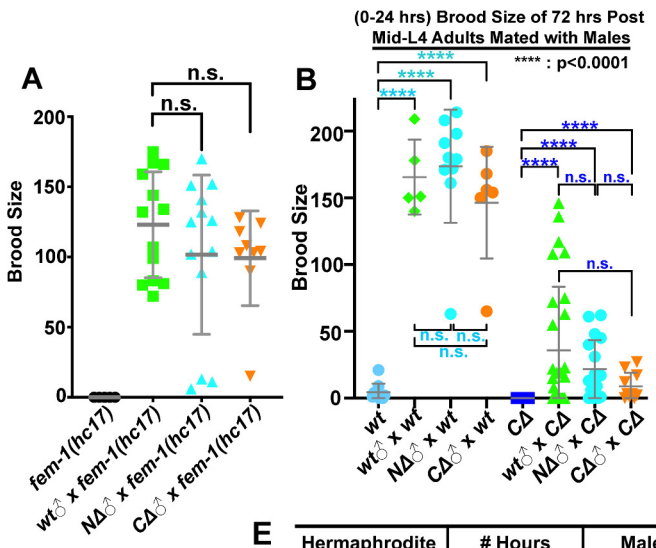

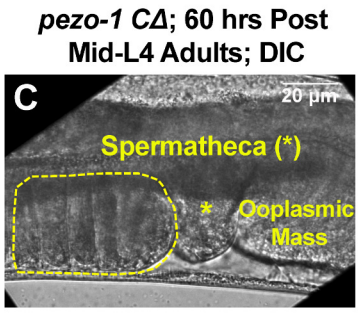

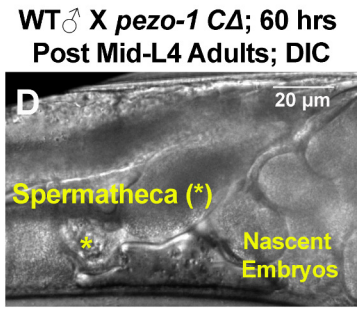

E

Hermaphrodite Genotype	# Hours Post Mid-L4	Male Genotype	# Ovulations per hour	# Tested Gonad Arms
Wild Type	24 hours	N.A.	2.29 ± 0.92	17
pezo-1 CΔ	24 hours	N.A.	1.36 ± 0.74	33
Wild Type	48 hours	N.A.	1.72 ± 1.10	25
Wild Type	48 hours	*him-8*	1.80 ± 0.92	10
Wild Type	48 hours	*spe-9 (hc52ts); him-8*	2.00 ± 1.31	15
pezo-1 CΔ	48 hours	N.A.	0.25 ± 0.44	20
pezo-1 CΔ	48 hours	*him-8*	1.50 ± 1.09	12
pezo-1 CΔ	48 hours	*spe-9 (hc52ts); him-8*	1.50 ± 0.76	14

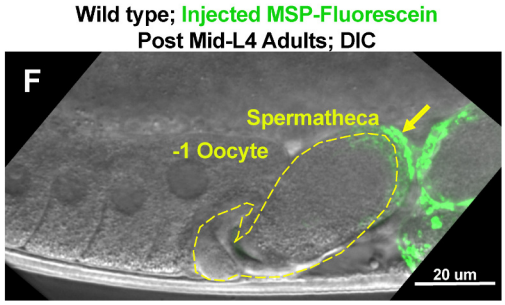

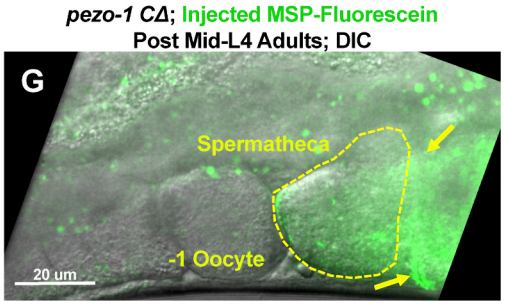

H

Hermaphrodite Genotype	# Hours Post Mid-L4	Male Genotype	# Ovulations per hour	# of Gonads tested
Wild Type	48 hours	N.A.	1.83 ± 0.98	6
Wild Type	48 hours	MSP::Fluorescein	1.1 ± 0.60	15
pezo-1 CΔ	48 hours	N.A.	0.25 ± 0.46	20
pezo-1 CΔ	48 hours	MSP::Fluorescein	1.83 ± 0.75	6

Figure 6. Male sperm rescue the ovulation defects in *pezo-1* mutants. (**A**) Both *pezo-1 CΔ* and *NΔ* males are fertile and sire progeny when mated with *fem-1(hc17ts)* mutants (essentially female animals). (**B**) Mating with male sperm rescued fertility in Day 3 *pezo-1 CΔ* adults (72 hr post mid-L4). (**C**) The oocyte maturation and ovulation rate are very low in Day 3 *pezo-1 CΔ* mutant adults, and oocytes accumulate in the proximal gonad arm (yellow dashed circle). (**D**) By contrast, the ovulation rates are recovered to high levels after mating with wildtype male sperm. Newly fertilized embryos pushed the ooplasmic mass out of the uterus. Yellow asterisks indicate the spermatheca (**C, D**). (**E**) Quantification of the oocyte ovulation rate of wildtype and *pezo-1 CΔ* adults at different ages. *him-8(e1489)* and *spe-9 (hc52ts)* sperm significantly rescue ovulation rates in *pezo-1 CΔ* hermaphrodites, even though they do not fertilize oocytes. (**F, G**) Injection of purified fluorescein-tagged MSP in the uteri of both wildtype and *pezo-1 CΔ* aged adults.

Figure 6 continued on next page

Figure 6 continued

Fluorescein-tagged MSP moved through the entire uterus to localize next to the spermatheca. The yellow dotted circle represents the spermatheca. The yellow arrows indicate the fluorescein-tagged MSP (green) localized next to the spermatheca. (**H**) Quantification of the oocyte ovulation rate of wildtype and *pezo-1 CΔ* adults without or without injections of fluorescein-tagged MSP. P-values: ****, p<0.0001 (*t*-test). Scale bars are shown in panels (C, D, F, G).

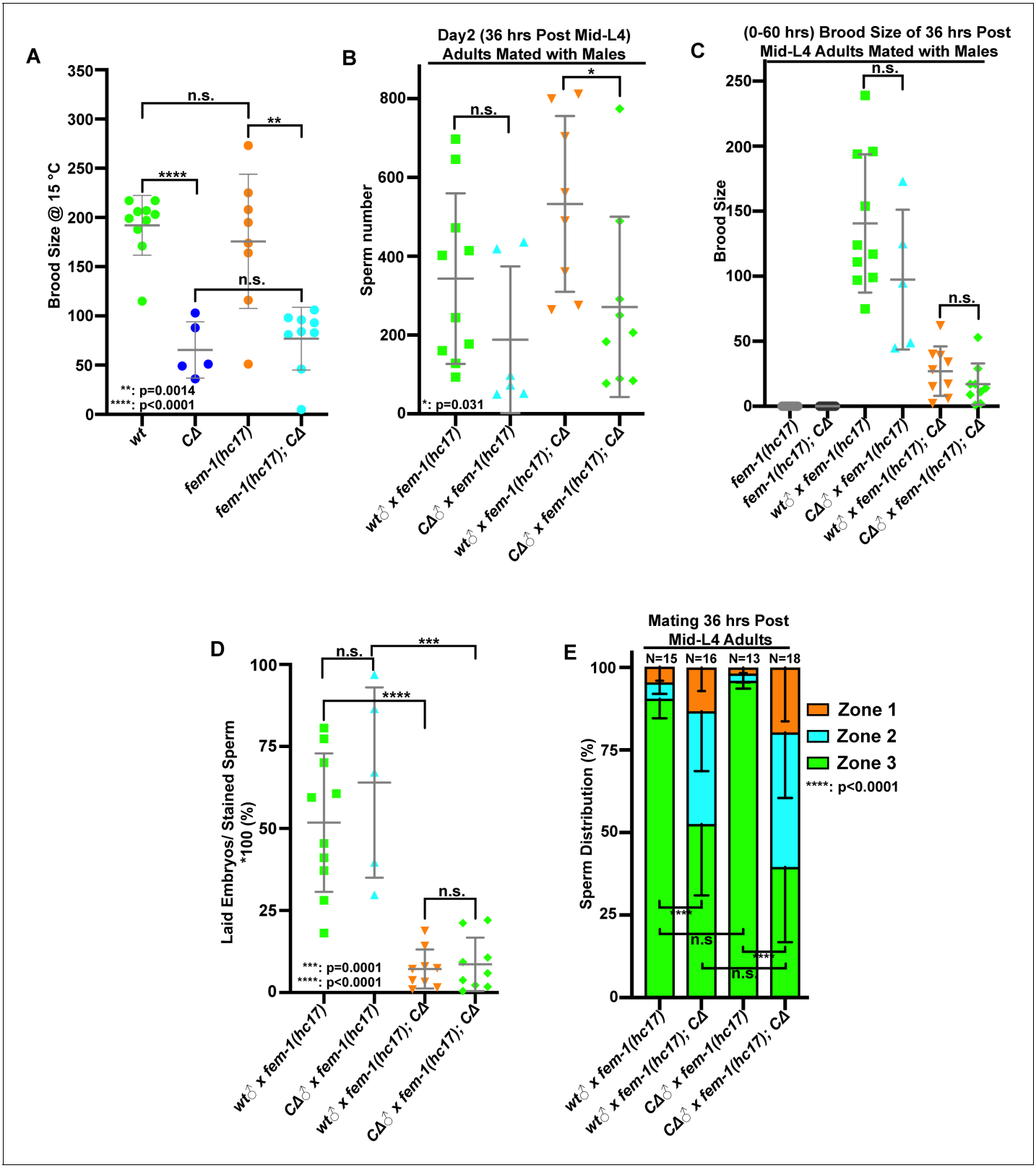

Figure 6—figure supplement 1. Male sperm rescue the fecundity in *pezo-1 CΔ* female. (**A**) Brood size was significantly reduced in *pezo-1 CΔ* females when compared with *fem-1(hc17)* females only at permissive temperature (15˚C). (**B**) Quantification of Mito-tracker-stained male sperm in the female uteri after mating for 30 min. (**C**) Both *pezo-1 CΔ* and wildtype males sire progeny when mated with *fem-1(hc17ts)* mutants (essentially female animals) and *pezo-1 CΔ* females at non-permissive temperature (25˚C). However, the number of cross progeny was greatly reduced in the *pezo-1 CΔ* female. (**D**)

Figure 6—figure supplement 1 continued on next page

Figure 6—figure supplement 1 continued

Fertilization ratio [(laid embryos/stained sperm) *100%] in different females. (**E**) Quantification of sperm distribution in the *pezo-1 C*Δ female after mating for 30 min. P-values: *, p=0.031 (**B**); **, p=0.0014 (**A**); ***, p=0.0001 (**D**); ****, p<0.0001 (**A, D, E**) (*t*-test).

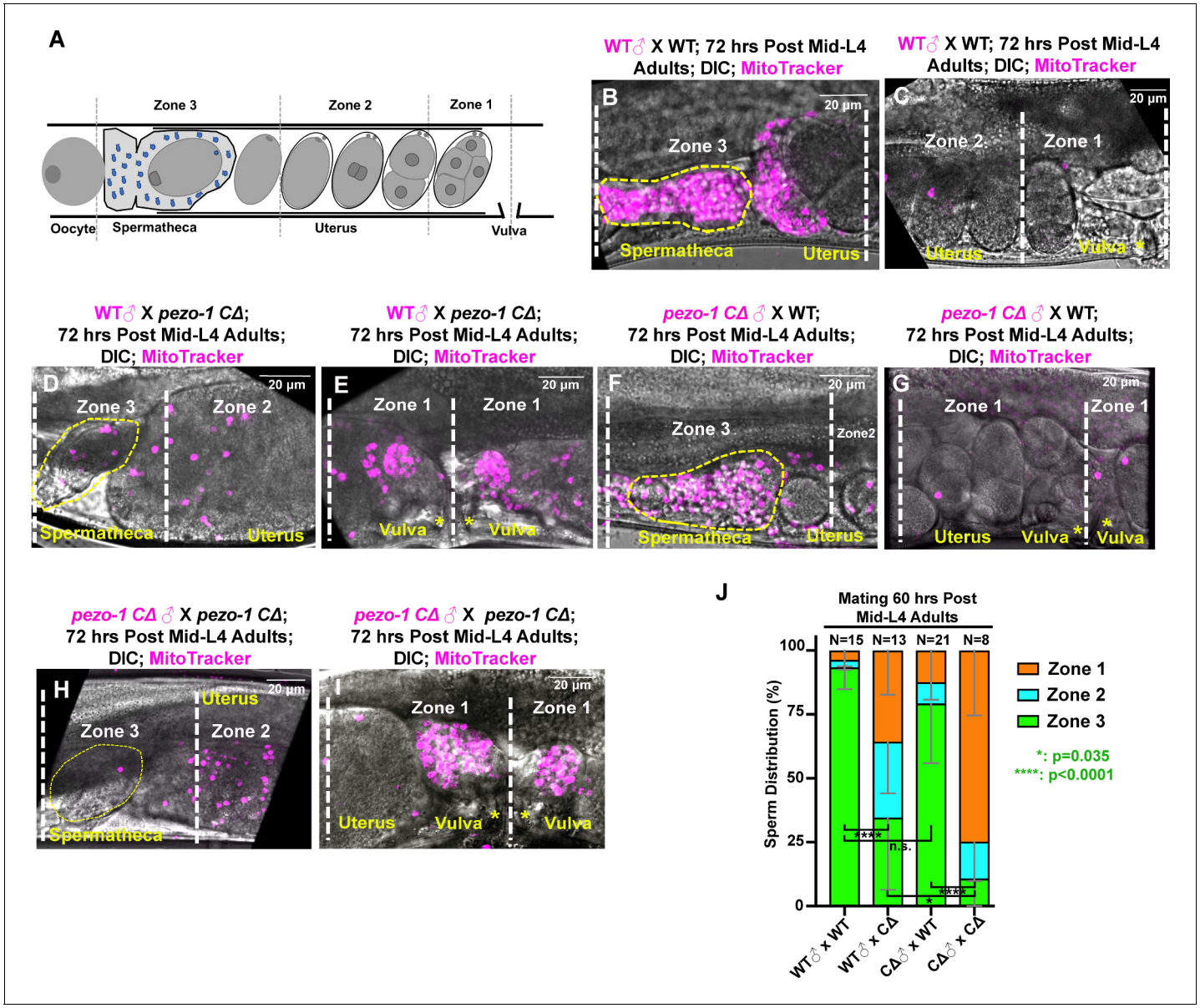

Figure 7. Sperm guidance and navigation is disrupted in *pezo-1* mutants. (**A**) To quantify sperm migration, this illustration indicates the three zones that were scored for sperm distribution. Zone 3 is the spermatheca region and the space containing the +1 fertilized embryo (yellow dotted circles in panels (B, **D, F, H**), whereas Zone 1 is the area closest to the vulva. Sperm distribution is measured 1 hr after males were removed from the mating plate. (**B–I**) The distribution of fluorescent male sperm labeled with MitoTracker in the three zones in both wildtype and *pezo-1* mutants 1 hr after the males were removed. Yellow asterisks indicate the vulva (**C, E, G, I**). Scale bars are indicated in each panel. (**J**) Quantification of sperm distribution values. The numbers of the scored uteri are shown above each of the bars. P-values: ****, p<0.0001 (*t*-test).

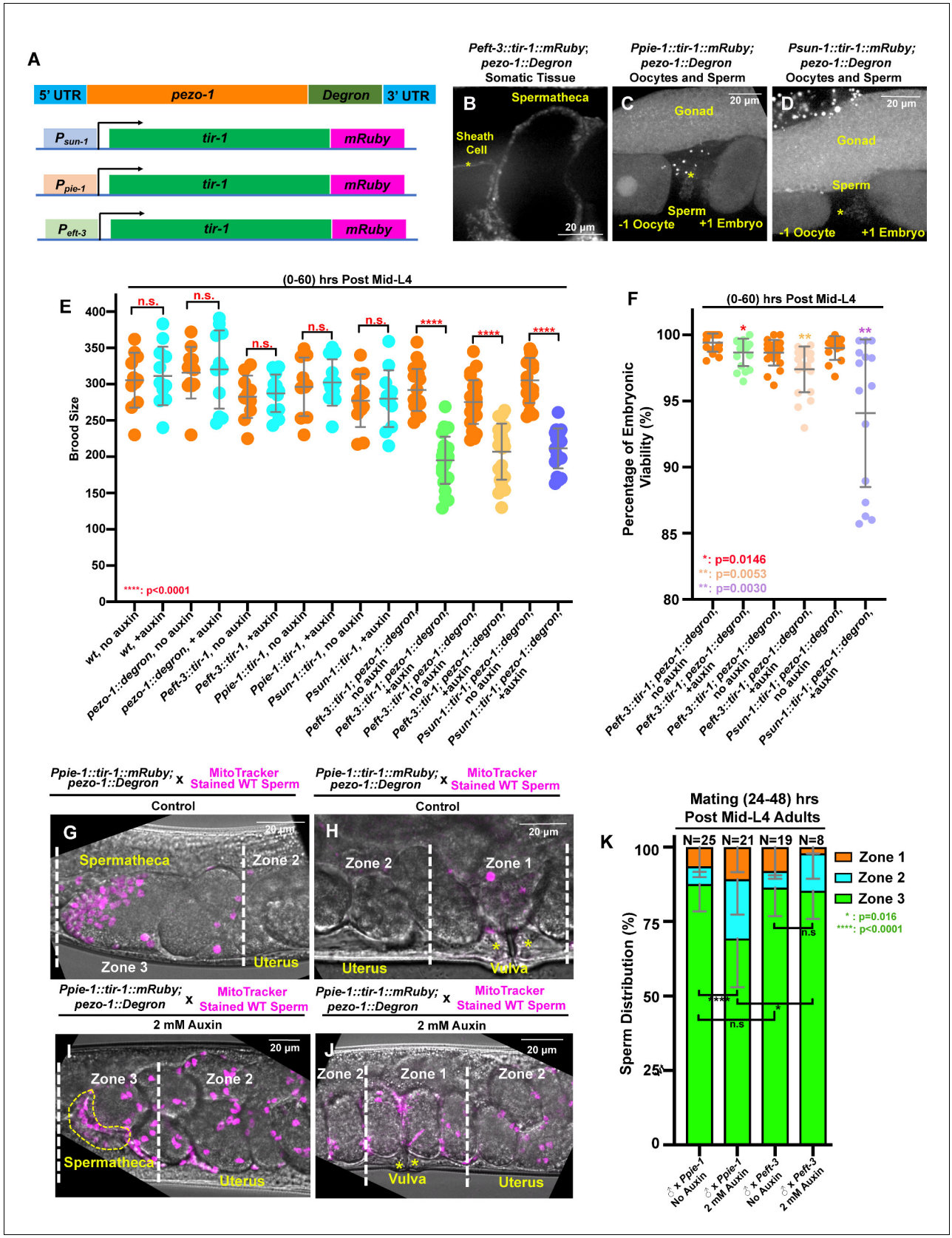

Figure 8. Tissue-specific degradation of PEZO-1 causes a reduced brood size and sperm navigational defects. (**A**) Schematic of the auxin-inducible degradation (AID) system. A degron tag was inserted at the 3′ end of the *pezo-1* coding sequence using CRISPR/Cas9-mediated editing. (**B**) The *eft-3*

Figure 8 continued on next page

Figure 8 continued

promoter was used to drive TIR-1 expression in most or all somatic tissues, including the spermatheca and the sheath cells. TIR-1::mRuby driven by the germline-specific promoters *sun-1* and *pie-1* is strongly expressed in the germline and oocytes (**C, D**), and weakly expressed in the sperm (asterisks in panels [C, D]). (**E, F**) Brood size and embryonic viability were reduced in all degron strains when animals were treated with 2 mM auxin. Data are presented as the mean ± standard error from at least two independent experiments. (**G–J**) Sperm distribution 1 hr after the removal of males from mating plates. The germline-specific PEZO-1::Degron hermaphrodites were mated with wildtype males for 30 min. The representative images show that *pezo-1* degradation in the germ line influences sperm distribution from the vulva (zone 1) to the spermatheca (zone 3). (**K**) Quantification of sperm distribution in the PEZO-1::Degron strains grown on plates with (+) or without (–) 2 mM auxin. P-values: *, p=0.0146 (**F**); *. p=0.016 (**K**); **, p=0.0030 (**F**); **, p=0.0053 (**F**); ****, p<0.0001 (**E, K**) (*t*-test). Scale bars are shown in each micrograph.

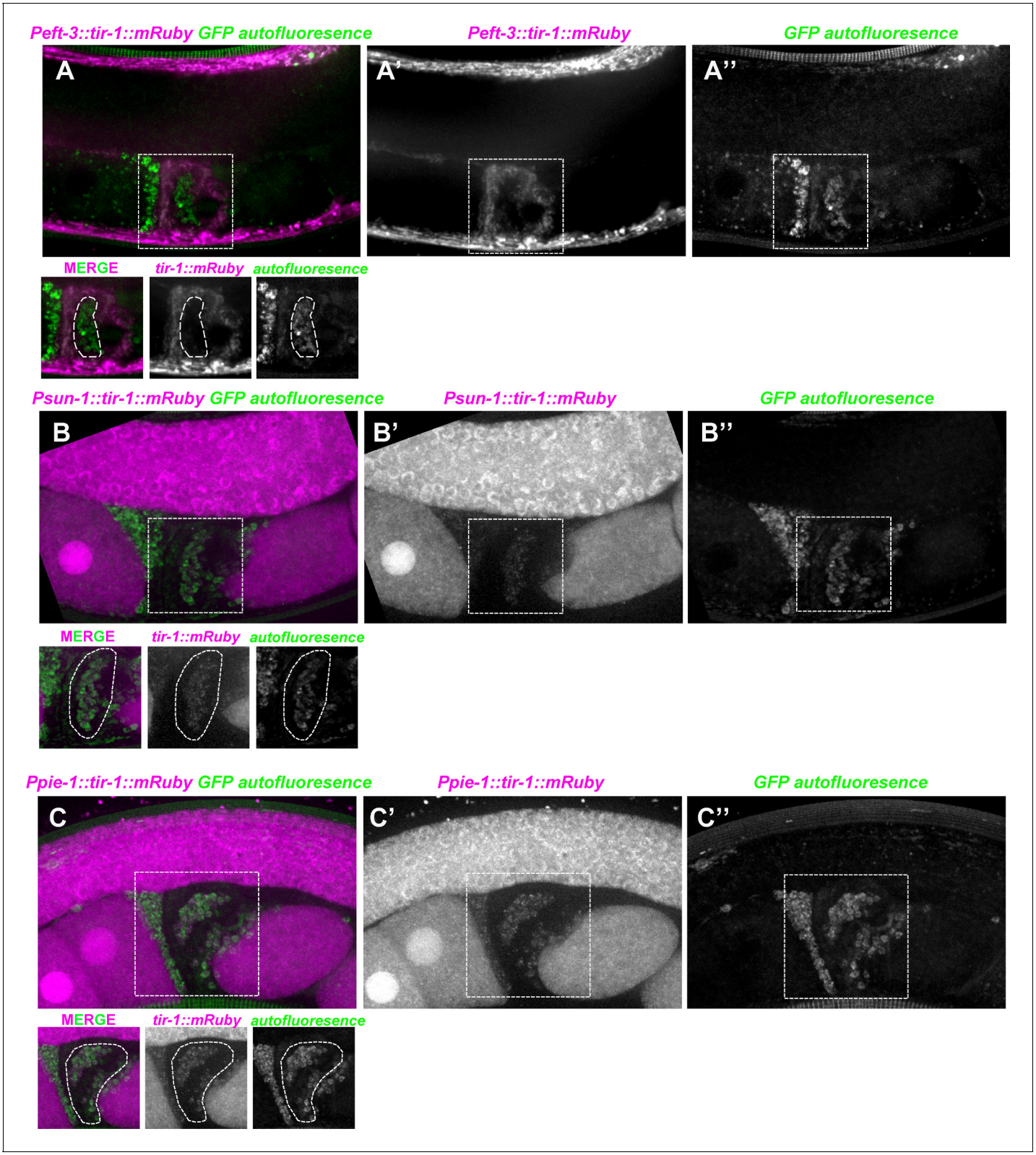

Figure 8—figure supplement 1. Expression pattern of *tir-1::mRuby* in reproductive tissues. (**A–A''**) The *eft-3* promoter was used to drive TIR-1 expression in most or all somatic tissues, including the spermatheca but not in the sperm [dotted circles in lower part of panel (A)]. Strong GFP autofluorescence is observed in the sperm cytosol (inserts from panels [**A, A''**]). (**B–C''**) TIR-1::mRuby driven by the germline specific promoters *sun-1* and *pie-1* is strongly expressed in the germline and oocytes (**B–B', C–C'**) and weakly expressed in the sperm (dotted circles in the inserts under panels [**B** and **C**]).

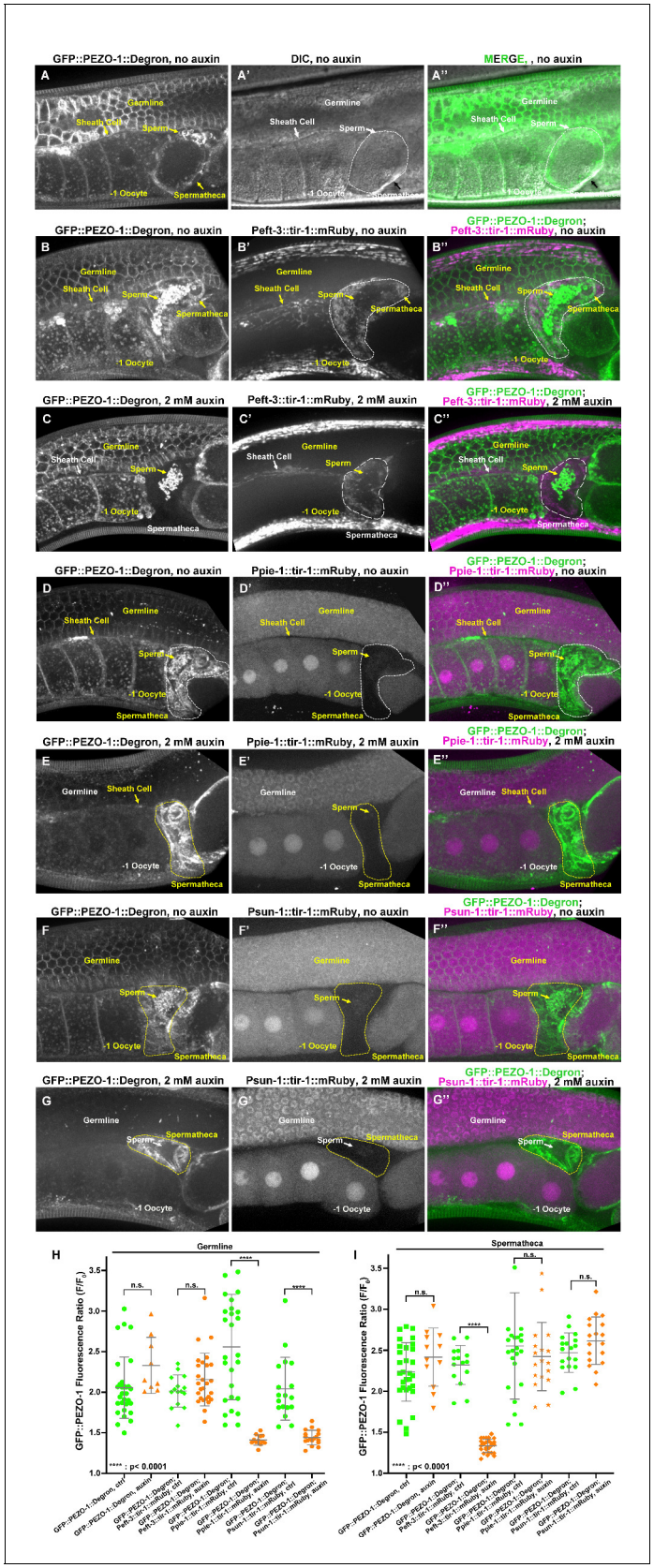

Figure 8—figure supplement 2. Tissue-specific degradation of PEZO-1 displays a reduced GFP::PEZO-1 fluorescence in each tissue expressing *tir-1::mRuby*. (**A–A''**) GFP::PEZO-1::Degron localized to reproductive tissues, such as the plasma membrane of the germline cells, oocyte, somatic sheath

Figure 8—figure supplement 2 continued on next page

Figure 8—figure supplement 2 continued

cells (yellow arrow, **A, A′′**), spermatheca (yellow arrow, **A, A′′**) and sperm. (**B–B′′**) TIR-1::mRuby driven by the somatic-tissue-specific promoter *eft-3* is strongly expressed in the somatic sheath cells and spermatheca. (**C–C′′, H–I**) Fluorescent signals of GFP::PEZO-1::Degron at spermatheca and somatic sheath cells are significantly reduced when animals were treated with 2 mM auxin. However, fluorescent signals of GFP::PEZO-1::Degron at germline cells, oocyte and sperm are not affected. (**D–E′′**) TIR-1::mRuby driven by the germline specific promoters *sun-1* and *pie-1* is strongly expressed in the germline and oocytes (**D′, E′, F, G′**). Fluorescent signals of GFP::PEZO-1::Degron in germline cells and oocytes were significantly reduced (**D–G, D′′–G′′, H–I**), whereas the expression level of GFP::PEZO-1::Degron in somatic tissues is not affected (**D–G, D′′–G′′, H–I**). (**H–I**) Quantification of the fluorescent signals of GFP::PEZO-1::Degron under the different conditions. P-values: ****, p<0.0001 (*t*-test).

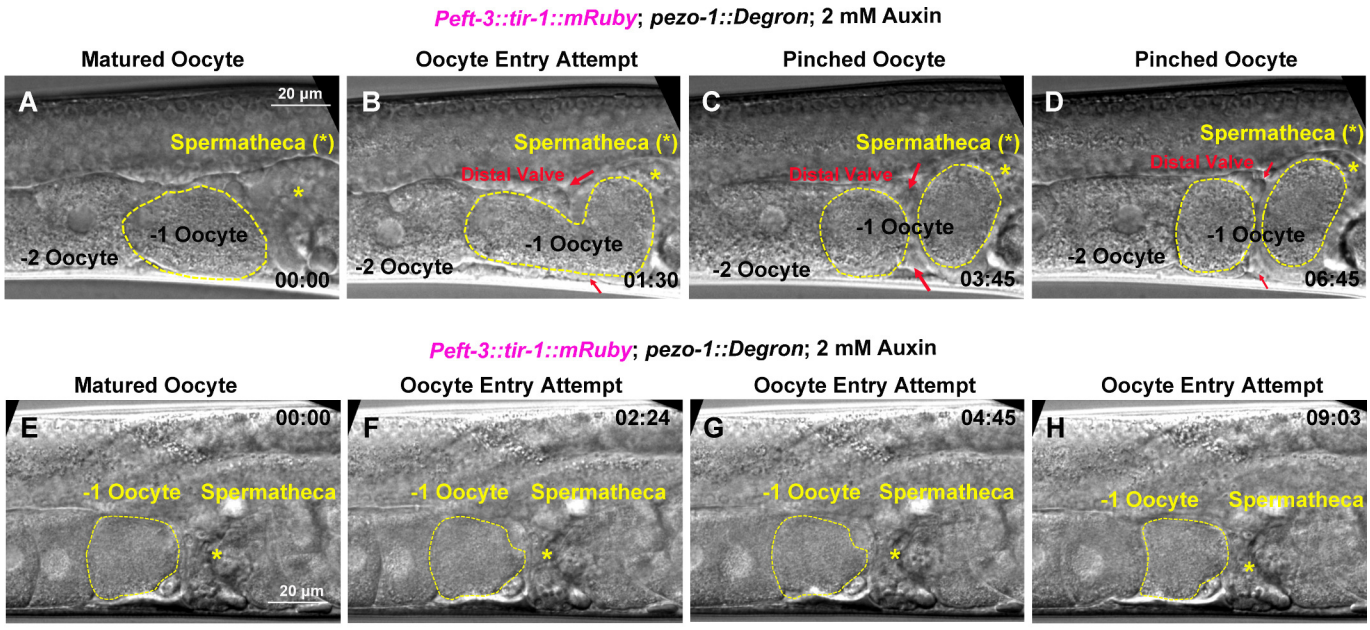

I

Genotype	Treatment	# Ovulations per hour	# Tested Gonad	# Pinched Oocyte	# Delayed Oocyte Entry
Peft-3::tir-1::mRuby; pezo-1::Degron	Control	1.71 ± 0.49	12	0% (0/13)	0% (0/13)
Peft-3::tir-1::mRuby; pezo-1::Degron	2 mM Auxin	1.14 ± 0.65	21	33.3% (9/27)	11.1% (3/27)

Figure 8—figure supplement 3. Somatic-tissue specific degradation of PEZO-1 causes severe ovulation defects. (**A–H**) Abnormal ovulations were observed in the somatic-tissue-specific PEZO-1::Degron animals. Two different ovulation events are shown. (**A, E**) Ovulation initiated by oocyte (yellow dotted circle) entry into the spermatheca. The spermathecal distal valve (red arrows) was defective (**B, C, E–H**) and either pinched off the oocyte when it attempted to enter the spermatheca (**B–D**) or failed to open and block/delayed the entry of the oocyte into the spermatheca (yellow asterisks) (**E–H**). The timing of each step is labeled in each panel in minutes and seconds. (**I**) Quantification of the oocyte ovulation rate and ovulation defects in the *Peft-3::tir-1; pezo-1::Degron* animals with or without 2 mM auxin. Scale bars are indicated in panels (A–H).

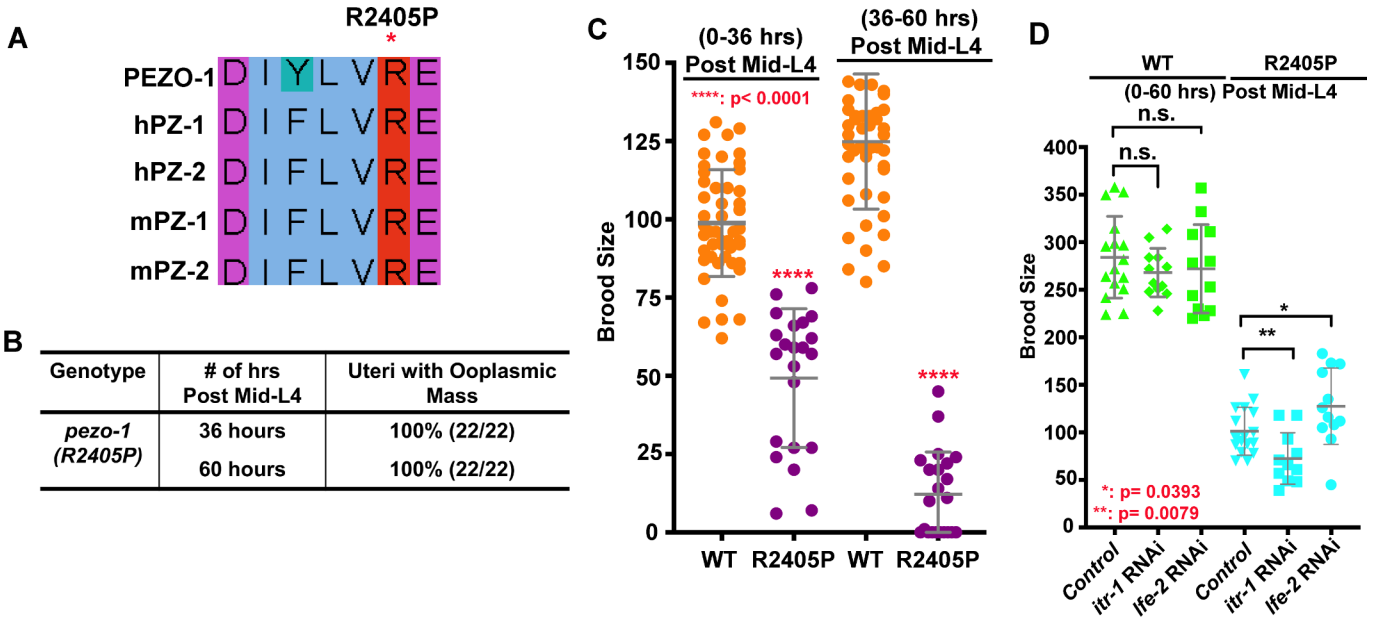

B

Genotype	# of hrs Post Mid-L4	Uteri with Ooplasmic Mass
pezo-1 (R2405P)	36 hours	100% (22/22)
	60 hours	100% (22/22)

E

Genotype	# Hours Post Mid-L4	Male Genotype	# Ovulations per hour	# Tested Gonad Arms
pezo-1 (R2405P)	24 hours	N.A.	2.17 ± 1.34	12
pezo-1 (R2405P)	48 hours	N.A.	0.10 ± 0.32	10
pezo-1 (R2405P)	48 hours	*spe-9 (hc52ts); him-8*	1.53 ± 0.92	16

Figure 9. The *PIEZO1* disease allele causes severe brood size reduction in *C. elegans*. (**A**) Sequence alignment showing arginine 2405 (R2405) in *C. elegans* PEZO-1 is highly conserved with human and mouse PIEZO1 and PIEZO2. (**B**) A conserved patient-specific allele, *pezo-1(R2405P)*, was generated and causes uterine ooplasmic masses and (**C**) a severe reduction in brood size. (**D**) *itr-1(RNAi)* enhanced the brood size reduction of *pezo-1(R2405P)* mutants, while *lfe-2(RNAi)* slightly rescued the reduced brood size. (**E**) *spe-9(hc52ts)* sperm rescued the very low ovulation rate in *pezo-1(R2405P)* hermaphrodites. P-values: *, p=0.0393 (**D**); **, p=0.0079 (**D**); ****, p<0.0001 (**C**) (*t*-test).

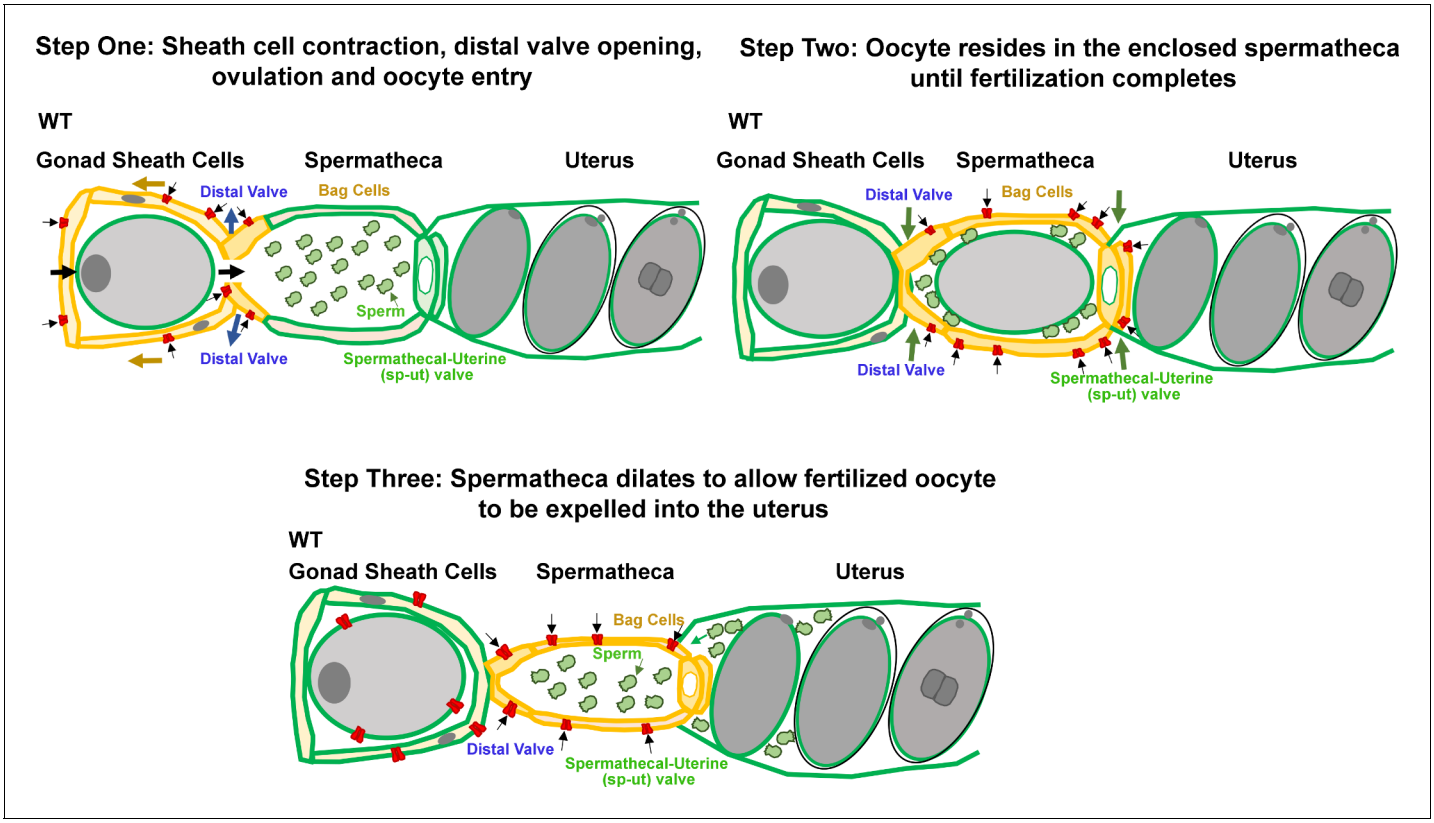

Figure 10. Working model for PEZO-1 during ovulation. Step One: PEZO-1 regulates somatic sheath cells and the spermathecal distal valve to push the oocyte into the spermatheca. Once a matured oocyte is ready for ovulation, PEZO-1 (red trapezoids) on the somatic sheath cells (yellow) triggers the contraction of the sheath to push the oocyte into the dilating spermatheca, through the distal valve. Meanwhile, the activated PEZO-1 (red trapezoids) on the distal valve (yellow) keeps the valve open and allows oocyte entry the spermatheca (green). Step Two: during fertilization, the PEZO-1 (red trapezoids) coordinates both distal (yellow) and spermathecal-uterine valves (yellow) to remain closed for 3–5 min. Step Three: After fertilization, PEZO-1 (red trapezoids) is activated on the spermathecal bag cells (yellow) and the sp-ut valve (yellow) to trigger a series of mechanical events (including spermathecal contractions and sp-ut valve opening) to expel the fertilized oocyte into the uterus (green). After oocyte entry into the uterus, we speculate that the PEZO-1 (red trapezoids) on the oocyte (far left) also functions to attract the sperm (green cells) back to the spermatheca. The precise mechanism of how PEZO-1 regulates sperm attraction remains unknown. Dysfunction of PEZO-1 causes the oocytes to be crushed as they are pushed into (Step 1) and expelled from the spermatheca (Step 3). The yellow represents the tissues that are under mechanical tension at each step during ovulation. PEZO-1 probably functions at the plasma membrane to sense the mechanical stimuli and to trigger intracellular signaling. The black arrows indicate the direction of extracellular cation influx when PEZO-1 channels are activated.